Future intensification of summer hypoxia in the tidal Garonne River (SW France) simulated by a coupled hydro sedimentary-biogeochemical model

Katixa Lajaunie-Salla, Aldo Sottolichio, Sabine Schmidt, Xavier Litrico, Guillaume Binet, Gwenaël Abril

Future intensification of summer hypoxia in the Tidal Garonne River (SW France) simulated by a coupled hydro sedimentary-biogeochemical model

Katixa Lajaunie-Salla[1,2], Aldo Sottolichio[1], Sabine Schmidt[1], Xavier Litrico[2], Guillaume Binet[2], Gwenaël Abril[1,3,4].

[1] Laboratoire EPOC, Environnements et Paléoenvironnements Océaniques et Continentaux UMR 5805, CNRS – Université de Bordeaux – Pessac, France

[2] LyRE, SUEZ research center, Bordeaux, France

[3] Departamento de Geoquímica, Universidade Federal Fluminense, Niterói, RJ, Brazil.

[4] Biologie des Organismes et Ecosystèmes Aquatiques (BOREA), Muséum National d'Histoire Naturelle, 61 rue Buffon, 75231, Paris cedex 05, France.

Corresponding Author: katixa.lajaunie@gmail.com

Acknowledgments

This study was funded by the Aquitaine Region and LyRE (SUEZ research center) who provided a PhD grant to K. Lajaunie-Salla. This research was also supported by the Cluster of Excellence COTE at the Université de Bordeaux (ANR-10-LABX-45). The authors are also grateful to the MAGEST network for the availability of data and to the SGAC and Bordeaux Metropole for providing urban effluent data and fruitful discussions.

Abbreviations

DO: dissolved oxygen
DOC: dissolved organic carbon
POC: particulate organic carbon
SSC: suspended sediment concentration
SO: sewage overflow
TGR: Tidal Garonne River
TMZ: turbidity maximum zone
WS: watershed
WW: wastewater
WWTP: wastewater treatment plant

Abstract

Projections for the next 50 years predict a widespread distribution of hypoxic zones in the open and coastal ocean due to environmental and global changes. Previously, the Tidal Garonne River (SW France) has experienced few episodic hypoxic events. However, predicted future climate and demographic changes suggest hypoxia could become more severe near the city of Bordeaux in the next few decades. A 3D model, which couples hydrodynamic, sediment transport and biogeochemical processes, is applied to assess the impacts of global and regional changes on oxygenation in the turbidity maximum zone (TMZ) of the Tidal Garonne River during low-discharge periods. The model predicts an intensification of summer hypoxia with an increase in temperature, a decrease in river flow or an increase in the local population but not with sea level rise, which has a negligible impact on dissolved oxygen. We tested different scenarios by combining these different factors according to the regional projections for 2050 and 2100. All simulations predict a spatial and temporal extension of summer hypoxia that needs to be considered by local water authorities to impose management strategies to protect the ecosystem.

Keywords: future changes, hypoxia, modeling, Tidal Garonne River, wastewater, water quality

1 Introduction

Climate models predict a general decrease in dissolved oxygen (DO) and a widespread distribution of hypoxia in the ocean (Cocco et al. 2013). Hypoxic waters are defined by a concentration of DO lower than 2 $mg.L^{-1}$ (or < 30% saturation, e.g., Rabalais et al. (2010)). Hypoxia exposes marine organisms to environmental stress and could have dramatic effects on coastal ecosystems; it increases fish mortality and consequently reduces the commercial fisheries (de Jonge et al. 2002; Vaquer-Sunyer and Duarte 2008). The comparison of observations between 1976 and 2000 has revealed a faster decline in DO concentrations in the coastal ocean than in the open ocean due to eutrophication (Gilbert et al. 2010).

Global change promotes coastal hypoxia due to a combination of different mechanisms. First, an increase in temperature decreases oxygen solubility in surface water and favors thermal stratification of the water column, which limits reaeration (Conley et al. 2009; Lehmann et al. 2014). Global models predict for the year 2100 an increase in oceanic water temperature of 2°C to 3°C (Cocco et al. 2013; IPCC 2013). In addition, Seneviratne et al. (2014) showed that future heat waves will be more frequent and intense than today. Water warming also accelerates biogeochemical processes that consume DO (Goosen et al. 1999). Second, global change affects coastal ecosystems by decreasing river flow in some regions and, more precisely, through an intensification of summer droughts. A reduction in summer river discharge is in fact due to a combination of climatic and anthropogenic factors including lower precipitation, hydroelectric power dams and irrigation within watersheds (Boé and Habets 2014). The river flow change could alter coastal estuarine tidal currents, sediment transport, and the transit and mineralization of terrestrial organic material in estuaries (Abril et al. 1999; Howarth et al. 2000). Third, climate models project a sea level rise between 0.5 and 1 m in 2100 (IPCC 2013). In estuaries, a consequence could be an increased propagation of the tide, leading to an upstream extension of the marine influence (Robins et al. 2016).

These climatic changes interact with the population and activity development in the coastal zone. Human activities enrich coastal waters with nutrients and organic matter (OM) and contribute to hypoxia through eutrophication (Diaz and Rosenberg 2008; Cotovicz et al. 2017). The organic matter of wastewater effluents is very labile and is quickly degraded, which consumes DO (Lajaunie-Salla et al. 2017). Wastewaters are also a source of ammonium that is nitrified in waters, which also consumes DO. The development of large cities in coastal areas thus has negative impacts on water quality (Zhao et al. 2015). For example, hypoxia events have been recorded in estuaries with nearby important urban areas such as the Thames Estuary (Tinsley 1998), the Yangtze Estuary (Li et al. 2002), and the Chesapeake Bay (Hagy et al. 2004).

In macrotidal estuaries, summer hypoxia is usually associated with the presence of a turbidity maximum zone (TMZ), which limits primary production and favors organic matter degradation (Thouvenin et al. 1994; Talke et al. 2009; Etcheber et al. 2011). Deoxygenation in a TMZ is the result of complex interactions between processes consuming oxygen, such as the degradation of organic matter or nitrification, and processes supplying oxygen, such as gas exchange at the water-air interface or the advection of DO-rich waters from upstream and downstream (Soetaert et al. 2006; Talke et al. 2009; Lanoux et al. 2013). These processes are highly variable in time, depending on hydrodynamics, particle settling/resuspension with semidiurnal and fortnightly tidal cycles (Abril et al. 1999), and sporadic storm overflow of urban water (Etcheber et al., 2011; Lanoux et al., 2013). Global and local changes are likely to increase temperature and wastewater discharges, to modify river flow and TMZ dynamics and, therefore, to amplify hypoxia events in macrotidal estuaries. However, this hypothesis needs to be quantified in order to allow preventive strategy management. For this purpose, it is necessary to estimate the expected minimum DO levels (DO_{min}), the duration and extension of future hypoxia events, and to identify the contribution of each forcing factor. This requires a model coupling hydrodynamic, sediment transport and biogeochemical processes to predict DO variations according to the environmental conditions (Talke et al. 2009; Peña et al. 2010; Testa et al. 2014). Numerical models are the only method to assess DO sensitivity to forcing factor variations and to test DO changes under scenarios of climate and local changes (Justić et al. 2007; Vanderborght et al. 2007; Cox et al. 2009; Wild-Allen et al. 2009; Skerratt et al. 2013). For example, a modeling study has shown that climate change could increase hypoxia events in the Oyster Grounds (North Sea) and that DO_{min} could decrease by 0.8 $mg.L^{-1}$ in 2100 (Meire et al. 2013). Such numerical models are also management tools to help water policymakers maintain good water quality in coastal environments (Kemp et al. 2009).

The objective of this work is to evaluate the potential impacts of global and local changes on the oxygenation of the Tidal Garonne River (SW France). Continuous monitoring data (Lanoux et al. 2013; Schmidt et al. 2017) have revealed that the Tidal Garonne River (TGR) had previously experienced few hypoxic events. However, continuing changes (temperature increase, increase in TMZ duration and concentration, development of the Bordeaux Metropolis) suggest that summer hypoxia near the city of Bordeaux could be more pronounced in the next decades. In this work, we use a recently developed 3D numerical model of dissolved oxygen (Lajaunie-Salla et al., 2017) to estimate the influence of the main identified factors likely to evolve in the next 50–100 years (fluvial discharge, temperature, urban development, and sea level rise) that may affect DO. The aim of the study is to simulate the probable future summer oxygenation according to the influence of these pressures, considered alone or combined, and to discuss the future risk of hypoxia in the TGR.

2 Materials and Methods

2.1 Study Area

The Gironde Estuary, located in southwestern France on the Atlantic coast, is formed by the confluence of the Garonne and the Dordogne Rivers. This macrotidal fluvio-estuarine system is characterized by the presence of a TMZ with suspended sediment concentration (SSC) > 1 $g.L^{-1}$ (Allen 1972). The TMZ is formed by the so-called tidal pumping effect (Uncles et al., 1985), consisting of mud trapping due to tidal asymmetry, i.e., the flood phase is shorter but with more intense currents than the ebb phase (Allen et al. 1980). The TMZ moves seasonally along the estuary axis according to fluvial discharges. In summer, when river flows decrease, the TMZ moves toward the tidal Dordogne and Garonne rivers, i.e., the portions of the rivers where the tidal waves propagate. A TMZ is present in the Tidal Garonne River between 3 and 8 months per year (Jalón-Rojas et al. 2015).

The Garonne River is the main tributary of the Gironde Estuary: it drains a watershed of 55 000 km^2; the mean annual discharge is 600 $m^3.s^{-1}$, ranging between extreme daily values of 54 and 4720 $m^3.s^{-1}$. The Bordeaux Metropolis is located 25 km from the confluence. The sewage system of the metropolis drains an urban surface area of 578 km^2 and serves a population estimated at 749 595 inhabitants in 2015. Two wastewater treatment plants (WWTPs, Clos de Hilde and Louis Fargue) continuously discharge treated wastewater into the TGR (Fig. 1); in addition, nine sewage overflows (SOs) occasionally discharge untreated wastewater into the TGR.

DO levels in the TGR are strongly influenced by water temperature, river flow, TMZ occurrence and urban effluents (Lajaunie-Salla et al., 2017; Lanoux et al., 2013; Schmidt et al., 2017). Hypoxia events preferentially occur during summer, when water temperature is increased to 24°C, a few days after a spring tide (Lanoux et al., 2013), as the result of an increased oxygen demand followed by reduced reaeration due to high turbidity (Lajaunie-Salla et al., 2017). Lajaunie-Salla et al. (2017) highlighted that wastewater effluents during deoxygenation events decreased the DO_{min} at Bordeaux by 10 %sat (~0.8 $mg.L^{-1}$). The projected development of Bordeaux Metropolis will lead to an increase in effluents, which would contribute to an intensification of the summer hypoxia in the Tidal Garonne River. To limit this risk in the TGR, a challenging objective of a minimum daily mean DO of 5 $mg.L^{-1}$ has been enforced by the local water agency to attain a good ecological status. Schmidt et al. (2017) highlighted that an increase of 2°C in summer leads to a daily average DO level below this threshold.

2.2 Model description

We used the three-dimensional SiAM-3D model coupling hydrodynamic, sediment transport and biogeochemical models recently developed by Lajaunie-Salla et al. (2017). The hydrodynamic and sediment transport models, initially developed by Brenon and Hir (1999) and Cugier and Le Hir (2002) for the Seine Estuary, were implemented in the Gironde Estuary by Sottolichio et al. (2000). The hydrodynamic model is based on the Navier-Stokes equations under the Boussinesq approximation and hydrostatic assumptions. The transport model solves the advection/dispersion equations for dissolved and particulate variables, i.e., suspended sediment, salinity and biogeochemical variables. For suspended sediment, the main cohesive sediment processes are taken into account to appropriately reproduce the dynamics of the TMZ (Van Maanen and Sottolichio, in revision). The hydrodynamic model is forced by tidal elevation at the shelf and by daily river flow of the Garonne and Dordogne Rivers at the upstream boundary (from French national hydrological data, www.hydro.eaufrance.fr).

We recently implemented the biogeochemical model for the Gironde Estuary to simulate biogeochemical processes that produce or consume oxygen in the water column, taking into account different types of dissolved and particulate organic matter (Lajaunie-Salla et al., 2017). These biogeochemical processes include the degradation of organic matter (mineralization of organic carbon and ammonification using the C/N ratio), nitrification, photosynthesis, respiration and mortality of phytoplankton, and DO gas exchange with the atmosphere. The model includes 11 state variables: dissolved oxygen (DO), ammonia (NH_4^+), nitrate (NO_3^-) and particulate and dissolved organic carbon (POC and DOC) from the watershed (POC from litter, DOC from rivers) and wastewater (from wastewater treatment plants and from sewage overflows), and POC from phytoplankton and detritus. The biogeochemical model requires inputs of the seasonal water temperature (data from MAGEST, a high-frequency water quality monitoring network, http://www.magest.u-bordeaux1.fr), wind and incident light intensity (from French meteorological office, Météo France). Urban wastewater discharge points are included in the model based on measurements provided by the operator of the sewer system, both regarding rejects of WWTP and SO (Fig.1).

The computational domain of the model extends from the 200 m isobath on the continental shelf to the upstream limits of the tidal propagation, at 170 km from the mouth (La Réole and Pessac-sur-Dordogne; Fig. 1) (Sottolichio et al. 2000). The 3D model is implemented for the Gironde Estuary on an irregular Cartesian grid with 2421 wet cells in the horizontal plane. In the vertical plane, the water column is split into 12 layers. The grid cell lengths progressively increase in the upstream direction from 500 m to 2 km. In the TGR, the width is described by three cells in the downstream section and by one cell in the upstream section. However, the average width and depth are rigorously well represented at all the cross sections along the tidal rivers, ensuring a good calculation of the oscillating volumes of water and tidal currents.

The originality of this biogeochemical model is to rely on extensive local data, particularly in the Tidal Garonne River. Except for nitrification, the degradation kinetics of different organic matter were measured for mixtures of estuarine turbid waters, riverine waters rich in phytoplankton or terrestrial litter, and domestic waters from SOs and WWTPs (Veyssy 1998; Lemaire et al. 2002; Etcheber et al. 2007; Lanoux et al. 2013).

In addition to temperature, the MAGEST network has recorded turbidity, salinity and DO every 10 minutes at different sites since 2005 (Fig. 1). The model was compared with data available for the TGR and tested on the basis of three criteria: i/ the ability to reproduce the observed DO variability at a seasonal scale; ii/ the ability to reproduce the spring-neap tidal cycle; and iii/ a statistical evaluation based on the Willmott skill score (WSS, Willmott (1982)). In summary, the model performed well (WSS > 0.7) in the lower TGR around Bordeaux but had lower performance levels at the upper section (WSS < 0.5) (for details, see Lajaunie-Salla et al. (2017)).

2.3 Reference year

The simulations were compared to a reference simulation, which corresponds to the year 2006 (Fig. 2). This year was chosen as a relatively critical reference simulation from the point of view of river discharge, temperature and hypoxia. The summer water temperature was on average 24.6°C, with a maximum of 29.4°C during a 21-day heat wave event. The mean summer Garonne River flow was 145 $m^3.s^{-1}$ (minimum of 54 $m^3.s^{-1}$) with 60 continuous days of river flow below 100 $m^3.s^{-1}$. In 2006, WWTP and DO discharges of urban water to the Garonne River were 51.2 and 9.6 Mm^3, respectively.

2.4 Scenarios

Different simulations were carried out to study the DO sensitivity of the Tidal Garonne River to the evolution of the main forcing factors: water temperature, river flow, sea level and population growth of Bordeaux Metropole. Present-day trends were used to extrapolate the expected values for 2050 and 2100:

- the water temperature increases following a mean rate of 0.06°C $year^{-1}$ (Le Treut 2013), suggesting an increase of +2°C in 2050 and +5°C in 2100;
- the mean Garonne river flow is expected to be reduced by 30 to 40% in 2050 and by 50 to 60% in 2100 (Etcheber et al. 2013; Schmidt et al. 2016);

- in the Bay of Biscay, the sea level has increased at a mean rate of 2 mm year^{-1} over the last few decades and should increase by 0.14 to 0.24 m in 2050 and by 0.28 to 0.48 m in 2100 (Le Treut, 2013);
- Bordeaux Metropolis is taking advantage of its attractiveness by implementing a dynamic policy to develop the city with the objective of reaching 1 million inhabitants by 2030 and then stabilizing the population until the end of the 21st century. (http://www.bordeaux-metropole.fr).

These expected trends were used to perform 14 simulations, including sensitivity analysis and two combined scenarios (Tab. 1), as follows:

- four simulations to test the impact of increasing temperature by adding a constant value (2, 3, 4 and 5°C) to the reference year (2006);
- four simulations to test the impact of a decrease in the Garonne flow, consisting of 78 days of constant river flow (100, 80, 60 and 40 $m^3.s^{-1}$) during the driest season, from July 15 to September 30. The selected values correspond to a decrease in the reference summer flow by 24%, 36%, 46% and 57%, respectively.
- three simulations to test the impact of sea level rise by +10, +20 and +40 cm.
- one simulation to test the impact of the increase in population assuming an associated increase in wastewater discharge by 50% and in a theoretical case of uncontrolled increase of urban discharges.
- the four forcing factors were combined to produce academic scenarios close to the expected scenarios for the years 2050 and 2100 (Table 1).

Each of the 14 simulations were run over 10 months, from January 1 to October 31. To form a TMZ, a stock of deposited mud was introduced in the estuary at the start of each simulation, which was easily resuspended during the first tidal cycle (see Lajaunie-Salla et al., 2017 for details). The mass of the TMZ was therefore the same for all the simulations, including those with a decreasing summer river flow, which did not significantly change the total mass of mud in the estuary. We used three quantitative indicators to assess the oxygenation state of the TGR waters: (1) the minimum DO value attained (DO_{min}); (2) the number of hypoxia days, i.e., DO < 2 $mg.L^{-1}$; and (3) the rates of biogeochemical processes consuming DO near Bordeaux and Portets, averaged for the summer months. The grid cells in front of Bordeaux and Portets were chosen because Bordeaux is under the impact of urban effluents and Portets represents the upstream presence of a TMZ.

3 Results and Discussion

3.1 Reference year

The reference simulation highlights the occurrence of the TMZ at Bordeaux from June to September, a summer DO decrease and two events of low DO, which were close to hypoxia (end of July and mid-September) (Fig. 2b). In fact, in summer, when the river flow decreases, the TMZ arrival in the tidal Garonne is always accompanied by a simultaneous decline in DO in Bordeaux waters (Etcheber et al., 2011; Schmidt et al, 2017). The lowest DOs occur at the end of July during a period characterized by a persistent low river flow, a heat wave and a sewage overflow discharge (Fig. 2). Moreover, as detailed in Lajaunie-Salla et al. (2017), the reference simulation shows that lower DO levels occur a few days after the spring tide peak and the deoxygenated zone moves between PK-10 and PK-20. In fact, at spring tide, the highest tidal currents promote resuspension and advection of suspended sediment, and the TMZ moves upstream of Bordeaux. Then, heterotrophic processes are favored and DO depletion is more intense in the upper TGR section than near Bordeaux. At neap tides, suspended matter settles, as well as organic matter coming from the watershed, and consequently reduces the mineralization of organic matter in the water column. Considering that at Bordeaux 32% of the DO consumption is due to wastewater effluents verses 4% at Portets (Lajaunie-Salla et al., 2017), at neap tides, DO depletion is more intense in Bordeaux waters than in the upper section of the TGR. In fact, in the area of Bordeaux, nitrification processes account for 19% of the DO consumption, and the watershed, 49%. Whereas in the area of Portets, nitrification accounts for 1% and the watershed for 95% of the DO consumption. At Bordeaux, the hypoxia threshold is not reached (DO > 2 $mg.L^{-1}$); however, at Portets, the hypoxia event lasted 3 days during this reference year (Tab. 2 & Fig. 4c).

3.2 Impact of increasing temperatures

The impact of an increase in temperature is negligible during winter and spring. From June, modeled scenarios show a reduction in DO_{min} at Bordeaux and Portets when the temperature is higher than 20°C (Fig. 3; Tab. 2). For a temperature increase of 5°C, at Bordeaux station, DO_{min} decreases from 28.9 to 14.3 %sat, and 26 days of hypoxia are simulated, whereas at Portets, DO_{min} decreases from 22.4 to 15.8 %sat, and 11 days of hypoxia are simulated (Tab. 2). At Bordeaux station, the deoxygenation observed in 2006 is amplified to hypoxia at the end of July when the temperature increases by +2°C. An increase of +4°C is required to observe hypoxia in mid-September (Tab. 2 and Fig. 3a).

In the area near Bordeaux, for the scenario of +2°C, DO consumption rates by nitrification and the mineralization of urban OM and watershed OM increase by 12%, 7% and 4%, respectively, whereas with an increase of 5°C, the consumption rates increase by 28%, 11% and 16%, respectively (Tab. 3). The results highlight that an increase in temperature affects biogeochemical processes and accelerates reactions. However, in the area of Portets, although the nitrification processes increase with temperature, DO consumption by urban OM decreases. This is explained by a more intense degradation of the urban OM close to its source, i.e., Bordeaux, leading to a lower amount of OM being transported to Portets.

3.3 Impact of population growth

The increase in wastewater discharge with demographic growth also results in lower DO values compared with those of the reference year only in summer (Fig. 3b). At Bordeaux, the model simulates 3 days of hypoxia with a DO_{min} of 23.6 %sat, whereas at Portets, urban effluents have less impact because DO_{min} decreases by only 1 %sat (DO_{min} = 21.3 %sat, Tab. 2). Close to Bordeaux, DO consumption due to urban OM degradation and nitrification increases by 50% and 42%, respectively (Tab. 3). At Portets, the same processes increase by 65% and 7%, respectively (Tab. 3), whereas the impact of the mineralization of OM from the watershed remains constant (Tab. 3). Population growth in Bordeaux Metropole moderately affects the oxygenation status of the TGR, despite the increase in urban labile organic matter inputs and then in DO consumption.

3.4 Impact of a long period of low river flow

Recent observations have shown an influence of the multidecadal discharge decrease on the intensification of the TMZ in the Tidal Garonne River (Jalón-Rojas et al., 2015). The model was thus used to test whether a discharge decrease also influences DO. The model simulates a marked saline intrusion (>4 at Bordeaux) and an obvious TMZ intensification and extension in the upper section of the TGR with a long period of low to very low water discharge (Fig. 4). DO_{min} decreases and the number of hypoxic days increases with the river flow reduction (Fig. 4; Tab. 2). This is explained by the TMZ development and its high SSC, which favors DO consumption by heterotrophic processes. Indeed, the strongest deoxygenation occurs when the river flow is the lowest and SSC is the highest (Fig. 4o). In the case of a discharge of 40 $m^3.s^{-1}$, a DO_{min} of 13.5 %sat and 8 %sat and 13 and 52 days of hypoxia are simulated at Bordeaux and Portets, respectively (Tab. 2). However, the comparison of low river flow scenarios suggests that heterotrophic processes are not the only controlling factor of DO distribution (Fig. 4). First, in the reference simulation, a short event of increasing river flow occurred at the end of July, which resulted in a temporary downstream relocation of a low-DO core near Bordeaux (Fig. 4c). For 100 $m^3.s^{-1}$, the hypoxia is also located close to Bordeaux, whereas the waters of the upper tidal river (PK -10 to -20) are still reoxygenated by fluvial inputs (Fig. 4f). In contrast, for the lowest simulated river flow (40 $m^3.s^{-1}$), the dilution of the upper Tidal Garonne River waters by oxygenated freshwaters becomes negligible, and then, several successive hypoxia events spread from PK-10 to PK-25 (Fig. 4o). This indicates that the upper section could be reoxygenated by the input of oxygenated advected freshwater. At Bordeaux, hypoxia is reached for the four simulated scenarios, whereas at Portets, it occurs only when the river discharge is lower than 60 $m^3.s^{-1}$ (Tab. 2).

We calculated the input of oxygenated freshwater (with a typical DO concentration of approximately 90 %sat) introduced by the Garonne River into the tidal river during a semidiurnal tidal cycle: the volume is 4.3 10^6 m^3 for a discharge of 100 $m^3.s^{-1}$, and 1.7 10^6 m^3 for 40 $m^3.s^{-1}$. This represents 3.8 and 1.5% of the average water volume between La Réole (the river end-member) and Bordeaux; and 22% and 9.3% of the averaged volume between La Réole and Portets (Fig. 1). The time to renew half of the water volume is shorter at Portets (between 1.1 and 2.7 days) than at Bordeaux (from 6.7 to 16.3 days). At Bordeaux, a water initially at 30 %sat would increase after one tidal

cycle by +2.3 %sat for a river flow of 100 $m^3.s^{-1}$, but only by +0.9 %sat for a river flow of 40 $m^3.s^{-1}$ (Portets, +13.2 %sat for 100 $m^3.s^{-1}$ and +5.6 %sat for 40 $m^3.s^{-1}$). Then, the fluvial DO renewal effect is reduced when the river flow decreases.

The last consequence of a lower fluvial discharge is an increase in DO consumption by nitrification and mineralization of OM from wastewater, whereas there is a decrease in the mineralization of OM from watersheds near Bordeaux and Portets (Tab. 3). This is a consequence of i/ a lower downstream dispersion of urban inputs, which tend to remain concentrated near Bordeaux and ii/ an upstream displacement of the TMZ to the upper section (PK-25, Fig. 4). The strongest deoxygenation observed for the simulation of a river flow of 40 $m^3.s^{-1}$ is thus a consequence of combined factors: reduced wastewater dispersion and dilution with oxygenated freshwaters and an increase in heterotrophic processes in the uppermost section where large amounts of fine sediments are trapped during summer.

3.5 Impact of sea level rise

Finally, we tested the potential impact of sea level rise (SLR) on DO. The simulations do not show a clear trend among the 3 scenarios (+10 cm; +20 cm; +40 cm) (Fig. 5). In the simulation SLR+10 cm, the TMZ is intensified and DO_{min} decreases from 28.9%sat to 25.6%sat at Bordeaux, but never reach the hypoxia threshold (Tab.2). At Portets the impact seems more critical with a DOmin decline from 22.4 %sat to 15.0 %sat, reaching 5 days of hypoxia (instead of 3 days for the reference year, Tab.2). But, surprisingly, in the simulation SLR+20 cm, the trend is reversed: the TMZ is attenuated and DO_{min} remains similar to the reference year values, with only two days of hypoxia at Portets (Tab.2). For the scenario SLR+40 cm, there is an amplification of deoxygenation at Portets: DO_{min} decreases at 14.7% and hypoxia occurs 6 days (Tab.2). The intensification of hypoxia for a sea level rise of 10 cm and 40 cm is explained by an increase of the tidal range and asymmetry in the Tidal Garonne River due to an overall higher depth, as observed in other urbanized estuaries (Winterwerp et al., 2013). These changes in tide are likely to increase the tidal pumping effect and therefore sediment resuspension and upstream transport (Winterwerp et al., 2013). For the simulation SLR+20 cm, flood dominance increases also, but simulated SSC decreases, which creates better conditions for oxygenation. As tidal currents are not expected to reduce, we hypothesize this could be attributed to a dilution effect due to a larger water volume in the tidal Garonne section (compared to SLR+10 cm). Indeed, the fate of suspended sediments in the water column of shallow tidal rivers results from a complex interaction between the tide, river flow, sediment supply and morphology (Robins et al., 2016). In particular, the evolution of the flood dominance depends on the relative importance of the local tidal range, the cross-section averaged depth, and the presence of channel and intertidal flats (Dronkers, 1986, Friedrichs et Aubrey, 1988). For the TGR, a sea level rise of approximately 20 cm seems to be a threshold value from which the effects of morphology and estuarine volume counteract the effects of increased tidal pumping and flood dominance. Then, at higher SLRs, the amplification of tidal pumping prevails over the dilution effect. Unfortunately, the description of lateral flats and channel bathymetry in the present model is not robust enough to make conclusions for these opposing effects. This implies the implementation of a morphodynamic model that more precisely describes the lateral flats and, eventually, the morphological evolution, which is far beyond the scope of the present study. Indeed, simulated results demonstrate this factor does not induce major changes in oxygenation compared with temperature and fluvial discharge changes (Tab. 2).

3.6 Scenarios of the combined effects for 2050 and 2100

To produce more realistic simulations, we combined the forcing factors to produce expected scenarios for 2050 and 2100. When compared to the reference scenario (Fig. 6a), the 2050 scenario shows no upstream TMZ migration nor extension, only a slight increase in SSC and a longer duration until October near Bordeaux (Fig. 6c). Simultaneously, there is a clear DO decrease and an increase in the hypoxia duration in Bordeaux (29 days). Conversely, the hypoxia threshold is never attained at Portets (Tab. 2). This is caused by two processes: the summer river flow is fixed at 80 $m^3.s^{-1}$, water in the upper sections is still reoxygenated by dilution with freshwater (Fig. 4i/6d), and there is no TMZ intensification (Fig. 6c).

For the 2100 scenario, the TMZ is far more concentrated until October compared with the reference, and it extends up to Portets in September (Fig. 6e). In the meantime, high and continuous DO depletion occurs over the entire section, from PK-15 to PK-25 (Fig. 6f). The extremely low summer river flow (40 $m^3.s^{-1}$) promotes an increased intensity and

duration of the TMZ. In addition, the input of well-oxygenated freshwater is limited, as already discussed in section 3.4. The duration of hypoxia increases at Bordeaux and Portets (91 and 78 days, respectively, Tab. 2). DO in the TGR decreases far below the threshold of 2 $mg.L^{-1}$ (DO_{min} at Bordeaux and Portets is less than 0.3 $mg.L^{-1}$) and almost reaches anoxia in early August (Tab. 2). Then, the hypoxia area extends over 40 km during the entire summer season. As these low DO values are modeled for surface waters, we assume a "dead zone" (Diaz and Rosenberg, 2008) could appear in the Tidal Garonne River near Bordeaux.

The average summer rates of biogeochemical processes impacting DO near Bordeaux and Portets show a significant increase (more than twice) in nitrification and degradation of urban OM in the 2050 and 2100 simulations due to the combined effect of increased temperature and population growth (Tab. 3). An increase in DO consumption rates of urban substrates (ammonia and urban matter) occurs for both scenarios (Tab. 3): in Bordeaux close to the urban source and at Portets 25 km upstream. In the case of Bordeaux, DO consumption by wastewater organic matter is higher for the 2050 scenario than for 2100, probably due to a stronger upstream dispersion of urban effluents from Bordeaux to Portets (Tab. 3).

The presence of a permanent summer hypoxia may cause serious ecological problems in the TGR, and in particular could perturb benthic and pelagic fauna (Diaz and Rosenberg 2008; Vaquer-Sunyer and Duarte 2008). A permanent seasonal hypoxia could have serious repercussions for the downstream migration of juvenile fishes (shad or sturgeon) (Lanoux et al. 2014). These ecological problems could also impact the economy of the fishing sector. Moreover, the potential formation of a « dead zone » would have an impact on atmospheric chemistry, causing greenhouse gas emissions (Naqvi et al. 2010; Howarth et al. 2011).

4 Summary and conclusions

The newly developed 3D biogeochemical model of the Tidal Garonne River coupling hydrodynamic and sediment transport models was particularly useful for understanding the future evolution of DO under global and local changes. An increase in temperature accelerates oxygen consumption by biogeochemical reactions. Population growth supplies additional labile organic matter in the Tidal Garonne River. A reduction in the river flow during summer droughts reduces the dilution of estuarine water with oxygenated freshwater and the downstream dispersion of the TMZ. Sea level rise can intensify mud trapping and oxygen consumption, but the competition between dilution and tidal pumping remain unclear and need specific investigations with high-resolution models.

The simulations of the combined effects of temperature, river flow, sea level and urban effluent changes predict a probable critical to very critical hypoxic state of the Tidal Garonne River for 2050 and 2100. A severe and permanent summer hypoxia is likely to develop between Bordeaux and Portets, reaching DO levels close to anoxia and potentially causing substantial repercussions on the ecosystem. These model results indicate the need for management actions to maintain the water quality of the Tidal Garonne River in the future. Possible actions could be to provide low river flow support, while still minimizing the impact of population growth through even more stringent wastewater treatment objectives. Moreover, the DO response to fluvial discharge highlights the need to maintain river discharge at a minimal threshold during summer, for example, by improving the release of water stored in dams or by limiting irrigation in the watershed during drought periods.

5 References

Abril G, Etcheber H, Le Hir P, et al (1999) Oxic/anoxic oscillations and organic carbon mineralization in an estuarine maximum turbidity zone (The Gironde, France). Limnol Oceanogr 44:1304–1315

Allen GP (1972) Étude des processus sédimentaires dans l'estuaire de la Gironde. Université de Bordeaux, p.314.

Allen GP, Salomon J, Bassoullet P (1980) Effects of tides on mixing and suspended sediment transport in macrotidal estuaries. Sediment Geol 26:69–90

Boé J, Habets F (2014) Multi-decadal river flow variations in France. 691–708. doi: 10.5194/hess-18-691-2014

Brenon I, Hir P Le (1999) Modelling the Turbidity Maximum in the Seine Estuary (France): Identification of Formation. 525–544

Cocco V, Joos F, Steinacher M, et al (2013) Oxygen and indicators of stress for marine life in multi-model global warming projections. Biogeosciences 10:1849–1868. doi: 10.5194/bg-10-1849-2013

Conley DJ, Carstensen J, Vaquer-Sunyer R, Duarte CM (2009) Ecosystem thresholds with hypoxia. Hydrobiologia 629:21–29. doi: 10.1007/s10750-009-9764-2

Cotovicz LC, Knoppers BA, Brandini N, et al (2017) Aragonite saturation state in a tropical coastal embayment dominated by phytoplankton blooms (Guanabara Bay - Brazil). Mar Pollut Bull 0–1. doi: 10.1016/j.marpolbul.2017.10.064

Cox TJS, Maris T, Soetaert K, et al (2009) A macro-tidal freshwater ecosystem recovering from hypereutrophication: the Schelde case study. Biogeosciences 6:2935–2948. doi: 10.5194/bg-6-2935-2009

Cugier P, Le Hir P (2002) Development of a 3D Hydrodynamic Model for Coastal Ecosystem Modelling. Application to the Plume of the Seine River (France). Estuar Coast Shelf Sci 55:673–695. doi: 10.1006/ecss.2001.0875

Dronkers J (1986) Tidal asymmetry and estuarine morphology. Neth. J. Sea Res. 20, 117-131

de Jonge VN, Elliott M, Orive E (2002) Causes , historical development , effects and future challenges of a common environmental problem : eutrophication. 1–19

Diaz RJ, Rosenberg R (2008) Spreading dead zones and consequences for marine ecosystems. Science (80-) 321:926–929. doi: 10.1126/science.1156401

Etcheber H, Coupry B, Coynel A, et al (2013) Disponibility of surficial continental waters. In: Le Treut H (ed) Impact of climate change in the Aquitaine region. Scientific Report., resses Uni. Pessac, p 365

Etcheber H, Schmidt S, Sottolichio A, et al (2011) Monitoring water quality in estuarine environments: lessons from the MAGEST monitoring program in the Gironde fluvial-estuarine system. Hydrol Earth Syst Sci 15:831–840. doi: 10.5194/hess-15-831-2011

Etcheber H, Taillez A, Abril G, et al (2007) Particulate organic carbon in the estuarine turbidity maxima of the Gironde, Loire and Seine estuaries: origin and lability. Hydrobiologia 588:245–259. doi: 10.1007/s10750-007-0667-9

Friedrichs CT, Aubrey DG, (1988). Non-linear tidal distortion in shallow well-mixed estuaries: a synthesis. Estuar. Coast. Shelf Sci. 27, 521-545.

Gilbert D, Rabalais NN, Díaz RJ, Zhang J (2010) Evidence for greater oxygen decline rates in the coastal ocean than in the open ocean. Biogeosciences 7:2283–2296. doi: 10.5194/bg-7-2283-2010

Goosen NK, Kromkamp J, Peene J, et al (1999) Bacterial and phytoplankton production in the maximum turbidity zone of three European estuaries: the Elbe, Westerschelde and Gironde. J Mar Syst 22:151–171

Hagy JD, Boynton WR, Keefe CW, Wood K V. (2004) Hypoxia in Chesapeake Bay, 1950–2001: Long-term change in relation to nutrient loading and river flow. Estuaries 27:634–658. doi: 10.1007/BF02907650

Howarth R, Chan F, Conley DJ, et al (2011) Coupled biogeochemical cycles: eutrophication and hypoxia in temperate estuaries and coastal marine ecosystems. Front Ecol Environ 9:18–26. doi: 10.1890/100008

Howarth RW, Swaney DP, Butler TJ, Marino R (2000) Rapid Communication: Climatic Control on Eutrophication of the Hudson River Estuary. Ecosystems 3:210–215. doi: 10.1007/s100210000020

IPCC (2013) Climate Change 2013: The Physical Science Basis. Contribution of Working Group I to the Fifth Assessment Report of the Intergovernmental Panel on Climate Change. 1535

Jalón-Rojas I, Schmidt S, Sottolichio A (2015) Turbidity in the fluvial Gironde Estuary (southwest France) based on 10-year continuous monitoring: sensitivity to hydrological conditions. Hydrol Earth Syst Sci 19:2805–2819. doi: 10.5194/hess-19-2805-2015

Justić D, Bierman Jr. VJ, Scavia D, Hetland RD (2007) Forecasting Gulf ' s Hypoxia : The Next 50 Years ? Estuaries and Coasts 30:791–801

Kemp WM, Testa JM, Conley DJ, et al (2009) Coastal hypoxia responses to remediation. Biogeosciences Discuss 6:6889–6948. doi: 10.5194/bgd-6-6889-2009

Lajaunie-Salla K, Wild-Allen K, Sottolichio A, et al (2017) Impact of urban effluents on summer hypoxia in the highly turbid Gironde Estuary , applying a 3D model coupling hydrodynamics , sediment transport and biogeochemical processes. J Mar Syst 174:89–105. doi: 10.1016/j.jmarsys.2017.05.009

Lanoux A, Etcheber H, Schmidt S, et al (2013) Factors contributing to hypoxia in a highly turbid, macrotidal estuary (the Gironde, France). Environ Sci Process Impacts 15:585–595. doi: 10.1039/c2em30874f

Lanoux A, Lepage M, De Watteville J, et al (2014) Effects of hypoxia on the fish and crustacean fauna in the Gironde Estuary. In: The 46th International Liege Colloquium. Liege, Belgium

Le Treut H (2013) Impact of climate change in the Aquitaine region. Scientific Report., Presses Un. Pessac

Lehmann A, Hinrichsen HH, Getzlaff K, Myrberg K (2014) Quantifying the heterogeneity of hypoxic and anoxic areas in the Baltic Sea by a simplified coupled hydrodynamic-oxygen consumption model approach. J Mar Syst 134:20–28. doi: 10.1016/j.jmarsys.2014.02.012

Lemaire E, Abril G, De Wit R, Etcheber H (2002) Effet de la turbidité sur la dégradation des pigments phytoplanctoniques dans l'estuaire de la Gironde. Geoscience 334:251–258

Li D, Zhang J, Huang D, et al (2002) Oxygen depletion off the Changjiang (Yangtze River) Estuary. Sci China Ser D 45:1137. doi: 10.1360/02yd9110

Meire L, Soetaert KER, Meysman FJR (2013) Impact of global change on coastal oxygen dynamics and risk of hypoxia. 2633–2653. doi: 10.5194/bg-10-2633-2013

Naqvi SWA, Bange HW, Farías L, et al (2010) Marine hypoxia/anoxia as a source of CH_4 and N_2O. Biogeosciences 7:2159–2190. doi: 10.5194/bg-7-2159-2010

Peña M, Katsev S, Oguz T, Gilbert D (2010) Modeling dissolved oxygen dynamics and coastal hypoxia: a review. Biogeosciences … 6:9195–9256. doi: 10.5194/bgd-6-9195-2009

Rabalais NN, Levin LA, Turner RE, et al (2010) Dynamics and distribution of natural and human-caused coastal hypoxia. Biogeosciences 7:585–619. doi: 10.5194/bgd-6-9359-2009

Robins PE, Skov MW, Lewis MJ, et al (2016) Impact of climate change on UK estuaries: A review of past trends and potential projections. Estuar Coast Shelf Sci 169:119–135. doi: 10.1016/j.ecss.2015.12.016

Schmidt S, Bernard C, Escalier J-M, et al (2017) Assessing and managing the risks of hypoxia in transitional waters: a case study in the tidal Garonne River (South-West France). Environ Sci Pollut Res. doi: 10.1007/s11356-016-7654-5

Schmidt S, Etcheber H, Sottolichio A, Castaing P (2016) Le réseau MAGEST: bilan de 10 ans de suivi haute-fréquence de la qualité des eaux de l'estuaire de la Gironde. In: Schmitt FG, Lefevre A (eds) Mesures haute résolution dans l'environnement marin côtier. Presses du CNRS

Seneviratne SI, Donat MG, Mueller B, Alexander L V. (2014) No pause in the increase of hot temperature extremes. Nat Clim Chang 4:161–163. doi: 10.1038/nclimate2145

Skerratt J, Wild-Allen K, Rizwi F, et al (2013) Use of a high resolution 3D fully coupled hydrodynamic, sediment and biogeochemical model to understand estuarine nutrient dynamics under various water quality scenarios. Ocean Coast Manag 83:52–66. doi: 10.1016/j.ocecoaman.2013.05.005

Soetaert K, Middelburg JJ, Heip C, et al (2006) Long-term change in dissolved inorganic nutrients in the heterotrophic Scheldt estuary (Belgium, The Netherlands). Limnol Oceanogr 51:409–423

Sottolichio A, Hir P Le, Castaing P (2000) Modeling mechanisms for the stability of the turbidity maximum in the Gironde estuary, France. Proc Mar Sci 3:373–386

Talke SA, Swart HE, de Jonge VN (2009) An Idealized Model and Systematic Process Study of Oxygen Depletion in Highly Turbid Estuaries. Estuaries and Coasts 32:602–620. doi: 10.1007/s12237-009-9171-y

Testa JM, Li Y, Lee YJ, et al (2014) Quantifying the effects of nutrient loading on dissolved O2 cycling and hypoxia in Chesapeake Bay using a coupled hydrodynamic–biogeochemical model. J Mar Syst 139:139–158. doi: 10.1016/j.jmarsys.2014.05.018

Thouvenin B, Le Hir P, Romana LA (1994) Dissolved oxygen model in the Loire estuary. Chang fluxes estuaries Implica- tions from Sci to Manag Acad 169–178

Tinsley D (1998) The Thames estuary: a history of the impact of humans on the environment and a description of the current approach to environmental management. In: Attrill M (ed) A Rehabilitated Estuarine Ecosystem SE - 2. Springer US, pp 5–26

Uncles RJ, Elliott TCA, Weston SA (1985) Observed fluxes of water and suspended sediment in a partly mixed estuary. Estuar. Coast. Shelf Sci. 20, 147-167

Van Maanen B, Sottolichio A (in revision). Hydro- and sediment dynamics in the Gironde estuary (France): sensitivity to seasonal variations in river inflow and sea level rise. Continental Shelf Research.

Vanderborght J-P, Folmer IM, Aguilera DR, et al (2007) Reactive-transport modelling of C, N, and O2 in a river–estuarine–coastal zone system: Application to the Scheldt estuary. Mar Chem 106:92–110. doi: 10.1016/j.marchem.2006.06.006

Vaquer-Sunyer R, Duarte CM (2008) Thresholds of hypoxia for marine biodiversity. Proc Natl Acad Sci U S A 105:15452–15457. doi: 10.1073/pnas.0803833105

Veyssy E (1998) Transferts de matière organiques das bassins versants aux estuaires de la Gironde et de l'Adour (Sud-Ouest de la France). Université de Bordeaux, p.262.

Wild-Allen K, Herzfeld M, Thompson PA., et al (2009) Applied coastal biogeochemical modelling to quantify the environmental impact of fish farm nutrients and inform managers. J Mar Syst 81:134–147. doi: 10.1016/j.jmarsys.2009.12.013

Willmott CJ (1982) Some comments on the evaluation of model performance. Bull Am Meteorol Soc 63:

Winterwerp JC, Wang ZB, van Braeckel A, van Holland G, Kösters F (2013). Man-induced regime shifts in small estuaries-II: A comparison of rivers. Ocean Dynamics, 63(11–12), 1293–1306. doi:10.1007/s10236-013-0663-8

Zhao W, Zhu X, Sun X, et al (2015) Water quality changes in response to urban expansion: spatially varying relations and determinants. Environ Sci Pollut Res 22:16997–17011. doi: 10.1007/s11356-015-4795-x

Table 1: Forcing of the different scenarios simulated with the model.

Scenarios		Temperature	River flow	Water level	Wastewater flow
Reference	**Ref**	T 2006	$Q_{G/D}$ 2006	3.24 m	Q_{WW} 2006
Effect of temperature	**+2°C**	T2006 +2°C	$Q_{G/D}$ 2006	3.24 m	Q_{WW} 2006
	+3°C	T2006 +3°C	$Q_{G/D}$ 2006	3.24 m	Q_{WW} 2006
	+4°C	T2006 +4°C	$Q_{G/D}$ 2006	3.24 m	Q_{WW} 2006
	+5°C	T2006 +5°C	$Q_{G/D}$ 2006	3.24 m	Q_{WW} 2006
Effect of demographic growth	**+POP**	T2006	$Q_{G/D}$ 2006	3.24 m	Q_{WW} 2006 +50%
Effect of river flow	**100 $m^3.s^{-1}$**	T2006	$Q_{G/D}$ 2006; Q_G = 100 $m^3.s^{-1}$ from 15/07 to 30/09	3.24 m	Q_{WW} 2006
	80 $m^3.s^{-1}$	T2006	$Q_{G/D}$ 2006; Q_G = 80 $m^3.s^{-1}$ from 15/07 to 30/09	3.24 m	Q_{WW} 2006
	60 $m^3.s^{-1}$	T2006	$Q_{G/D}$ 2006; Q_G = 60 $m^3.s^{-1}$ from 15/07 to 30/09	3.24 m	Q_{WW} 2006
	40 $m^3.s^{-1}$	T2006	$Q_{G/D}$ 2006; Q_G = 40 $m^3.s^{-1}$ from 15/07 to 30/09	3.24 m	Q_{WW} 2006
Effect of sea level	**+10 cm**	T2006	$Q_{G/D}$ 2006	3.34 m	Q_{WW} 2006
	+20 cm	T2006	$Q_{G/D}$ 2006	3.44 m	Q_{WW} 2006
	+40 cm	T2006	$Q_{G/D}$ 2006	3.64 m	Q_{WW} 2006
Combined effect	**2050**	T2006 +2°C	$Q_{G/D}$ 2006; Q_G = 80 $m^3.s^{-1}$ from 15/07 to 30/09	3.44 m	Q_{WW} 2006 +50%
	2100	T2006 +5°C	$Q_{G/D}$ 2006; Q_G = 40 $m^3.s^{-1}$ from 15/07 to 30/09	3.64 m	Q_{WW} 2006 +50%

Table 2: Minimum simulated DO (in % of saturation and in $mg.L^{-1}$), the corresponding temperature and the number of hypoxia days in Bordeaux and Portets for each scenario.

Scenarios		Bordeaux				Portets			
		T (°C)	DO_{min} (%)	DO_{min} ($mg.L^{-1}$)	Days of hypoxia	T (°C)	DO_{min} (%)	DO_{min} ($mg.L^{-1}$)	Days of hypoxia
Reference	**Ref**	27.2	28.9	2.3	0	24	22.4	1.8	3
Effect of temperature	**+2°C**	29.2	22.8	1.7	5	26	18.9	1.5	7
	+3°C	30.2	19.8	1.5	9	27	18.5	1.4	8
	+4°C	31.2	17.0	1.2	15	28	16.5	1.3	13
	+5°C	32.2	14.3	1.0	26	29	15.8	1.2	14
Effect of demographic growth	**+POP**	27.2	23.6	1.9	3	24	21.3	1.7	4
Effect of river flow	**100 $m^3.s^{-1}$**	26.9	23.7	1.9	4	24	33.5	2.8	0
	80 $m^3.s^{-1}$	26.8	19.5	1.5	8	23.7	32.2	2.7	0
	60 $m^3.s^{-1}$	26.8	15.6	1.2	11	24.4	19.5	1.6	12
	40 $m^3.s^{-1}$	27.4	13.5	1.0	13	24.4	8	0.7	52
Effect of sea level	**+10 cm**	27.2	25.6	2.0	0	23.1	15	1.2	5
	+20 cm	26.4	33	2.6	0	24.6	22.5	1.9	2
	+40 cm	23.7	29.7	2.3	0	22.6	14.7	1.2	6
Combined impact	**2050**	28.9	14	1.1	29	26.7	29.1	2.4	0
	2100	32.4	2.8	0.2	91	29.7	3.4	0.3	78

Table 3: Differences (in %) of biogeochemical process rates impacting DO between the scenarios and reference simulations during summer at Bordeaux.

Scenarios		Bordeaux			Portets		
		nitrification	mineralization TOC_{WS}	mineralization TOC_{WW}	nitrification	mineralization TOC_{WS}	mineralization TOC_{WW}
Effect of temperature	**+2°C**	+12%	+7%	+4%	+15%	-3%	-2%
	+3°C	+17%	+11%	+6%	+22%	-2%	-7%
	+4°C	+23%	+13%	+9%	+30%	-3%	-11%
	+5°C	+28%	+16%	+11%	+37%	-2%	-15%
Effect of demographic growth	**+POP**	+42%	-1%	+50%	+7%	-3%	+65%
Effect of river flow	**100 $m^3.s^{-1}$**	+8%	-1%	+4%	-4%	-8%	+20%
	80 $m^3.s^{-1}$	+25%	0	+3%	+15%	-9%	+29%
	60 $m^3.s^{-1}$	+45%	-4%	+6%	+67%	-14%	+41%
	40 $m^3.s^{-1}$	+66%	-14%	+6%	+159%	-18%	+52%
Effect of sea level	**+10 cm**	+3%	+3%	-7%	+4%	-4%	+14%
	+20 cm	0	0	0	-26%	-19%	-5%
	+40 cm	+3%	-13%	-12%	+11%	+3%	+18%
Combined effect	**2050**	+86%	-8%	+59%	+44%	-5%	+65%
	2100	+144%	-28%	+52%	+241%	-15%	+131%

Figure 1: The Tidal Garonne River in southwestern France. "PK" denotes the distances in km from the city center of Bordeaux; the control grid cell at Bordeaux is at PK-4 and Portets is at PK-20. In insert A, the purple triangles represent the position of sewage overflows (SOs) and the green squares represent the position of wastewater treatment plants (WWTPs). The area in orange represents the area of Bordeaux where the biogeochemical fluxes are calculated. In inset B, the purple line represents the 200 m isobath.

Figure 2: Influencing factors of the reference simulation (year 2006): time series of river flow (a, $m^3.s^{-1}$), water temperature (b, °C), discharge of sewage overflow (SO) and of wastewater treatment plants (WWTPs) (c, $m^3.s^{-1}$), simulated DO saturation (d, %), and SSC (d, $g.L^{-1}$) and tidal range (d, m) from January 1 to October 31. In figure b, the blue line and the green area show the median and the envelope of measured temperature for the period 2005-2015, respectively.

Figure 3: Temporal evolution of DO_{min} (over tidal cycle in %sat) at Bordeaux, from January to October, according to the scenarios of temperature increases (from 2°C to 5°C, a) or population growth (b). The blue line represents the 2006 reference simulation.

Figure 4: Spatiotemporal evolution of simulated surface daily average parameters along the Tidal Garonne River section: salinity (left), SSC (middle, in $g.L^{-1}$) and DO (right, in %sat). The simulations correspond to the reference with a summer mean Garonne discharge of 145 $m^3.s^{-1}$ (a, b and c) and to the following four scenarios: 100 $m^3.s^{-1}$ (d, e and f), 80 $m^3.s^{-1}$ (g, h and i), 60 $m^3.s^{-1}$ (j, k and l) and 40 $m^3.s^{-1}$ (m, n and o). The y-axis represents the kilometric points, and the white lines represent Bordeaux and Portets.

Figure 5: Spatiotemporal evolution of simulated surface daily average parameters along the Tidal Garonne River section: salinity (left), SSC (middle, in $g.L^{-1}$) and DO (right, in %sat). The simulations correspond to the three scenarios of SLR: +10 cm (a, b and c), +20 cm (d, e and f) and +40 cm (g, h and i). The y-axis represents the kilometric points, and the white lines represent Bordeaux and Portets.

Figure 6: Spatiotemporal evolution of daily average surface SSC (left, in $g.L^{-1}$) and DO (saturation, right in %) along the Tidal Garonne River section for the reference year 2006 (a and b) and the scenarios of 2050 (c and d) and 2100 (e and f). The y-axis represents the kilometric points, and the white lines represent Bordeaux and Portets.

Figure 1:

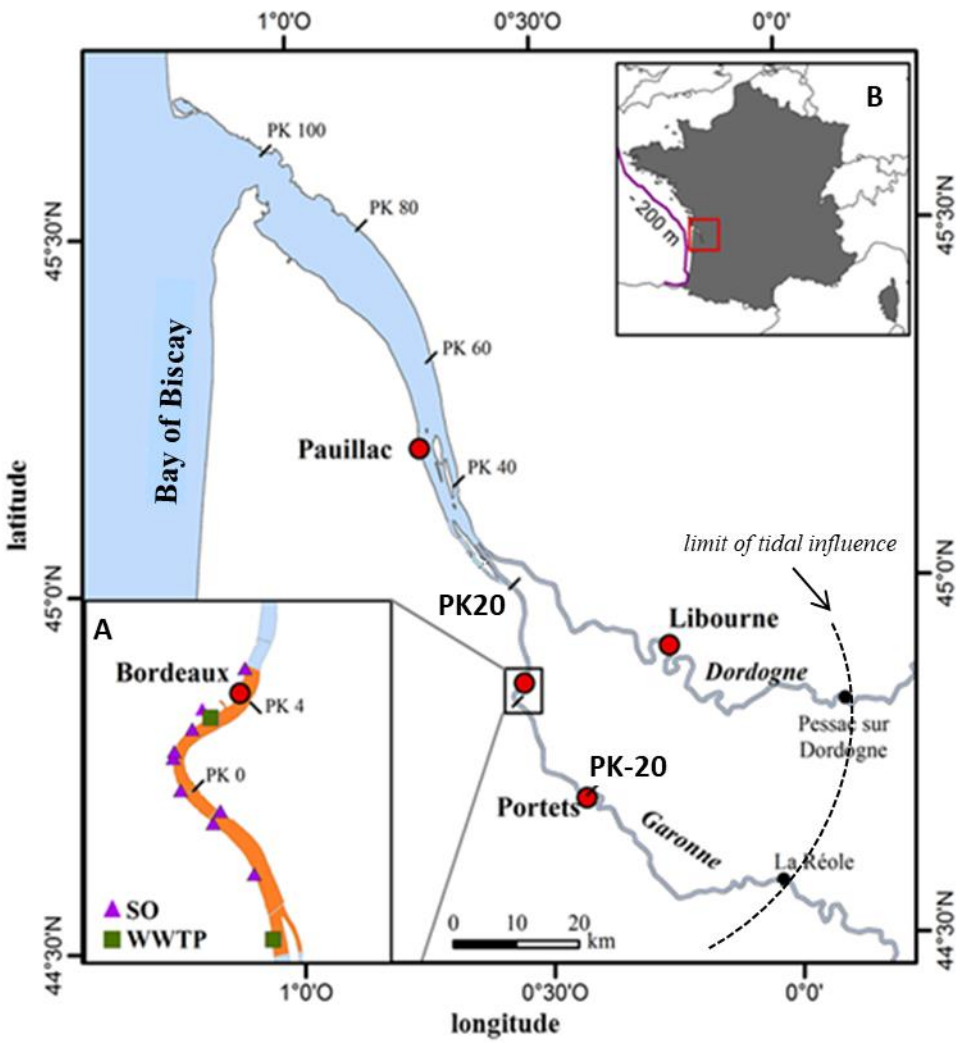
1°0'O
0°30'O
0°0'
45°30'N
45°0'N
44°30'N
latitude
longitude
Bay of Biscay
PK 100
PK 80
PK 60
PK 40
Pauillac
PK20
PK-20
Portets
Libourne
Dordogne
Pessac sur Dordogne
Garonne
La Réole
limit of tidal influence
B
- 200 m
A
Bordeaux
PK 4
PK 0
SO
WWTP
0 10 20 km

Figure 2:

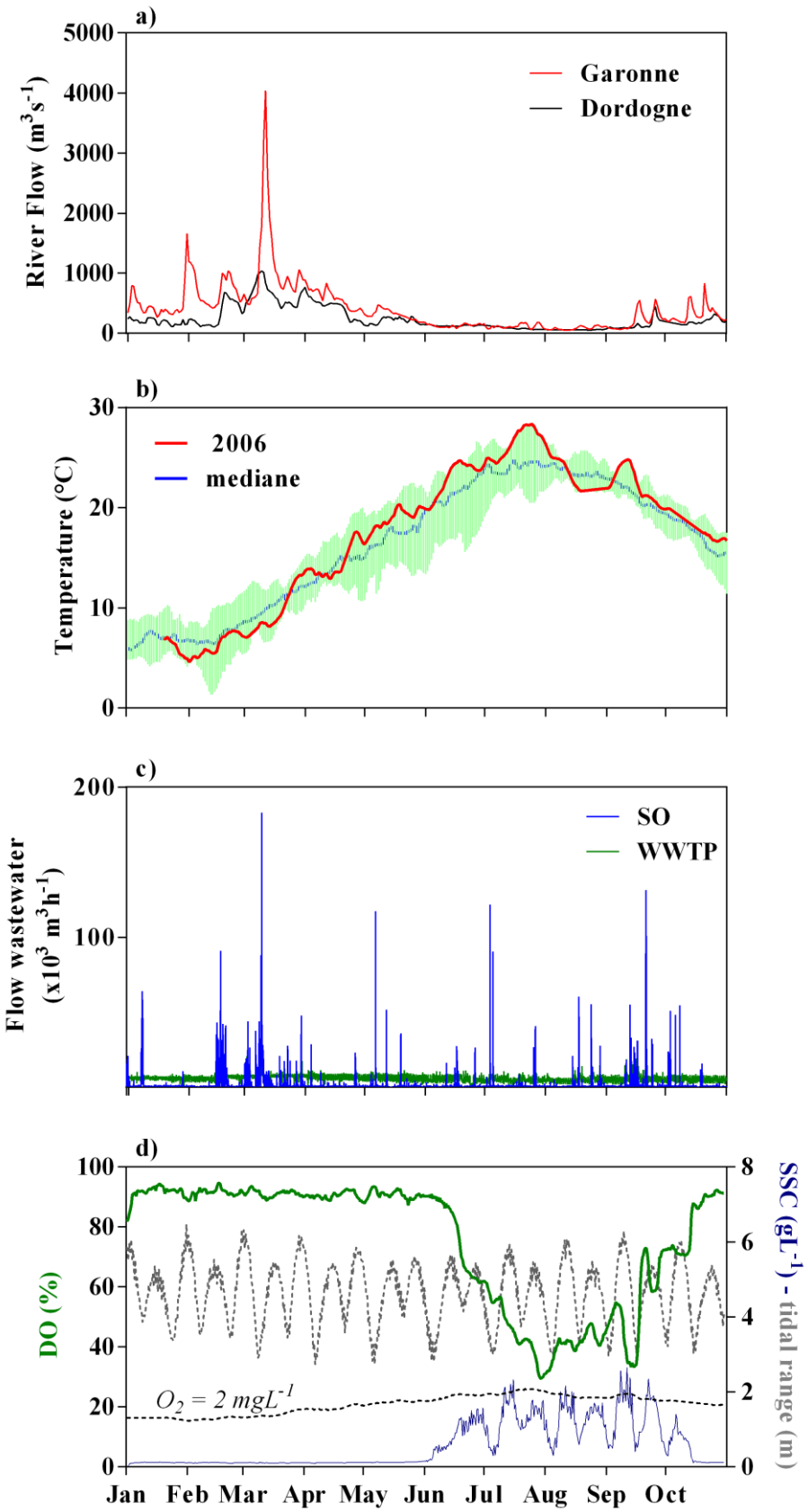
a)
River Flow (m^3s^{-1})
5000
4000
3000
2000
1000
0
Garonne
Dordogne
b)
Temperature (°C)
30
20
10
0
2006
mediane
c)
Flow wastewater ($x10^3$ m^3h^{-1})
200
100
SO
WWTP
d)
DO (%)
100
80
60
40
20
0
O_2 = 2 mgL^{-1}
SSC (gL^{-1}) - tidal range (m)
8
6
4
2
0
Jan Feb Mar Apr May Jun Jul Aug Sep Oct

Figure 3:

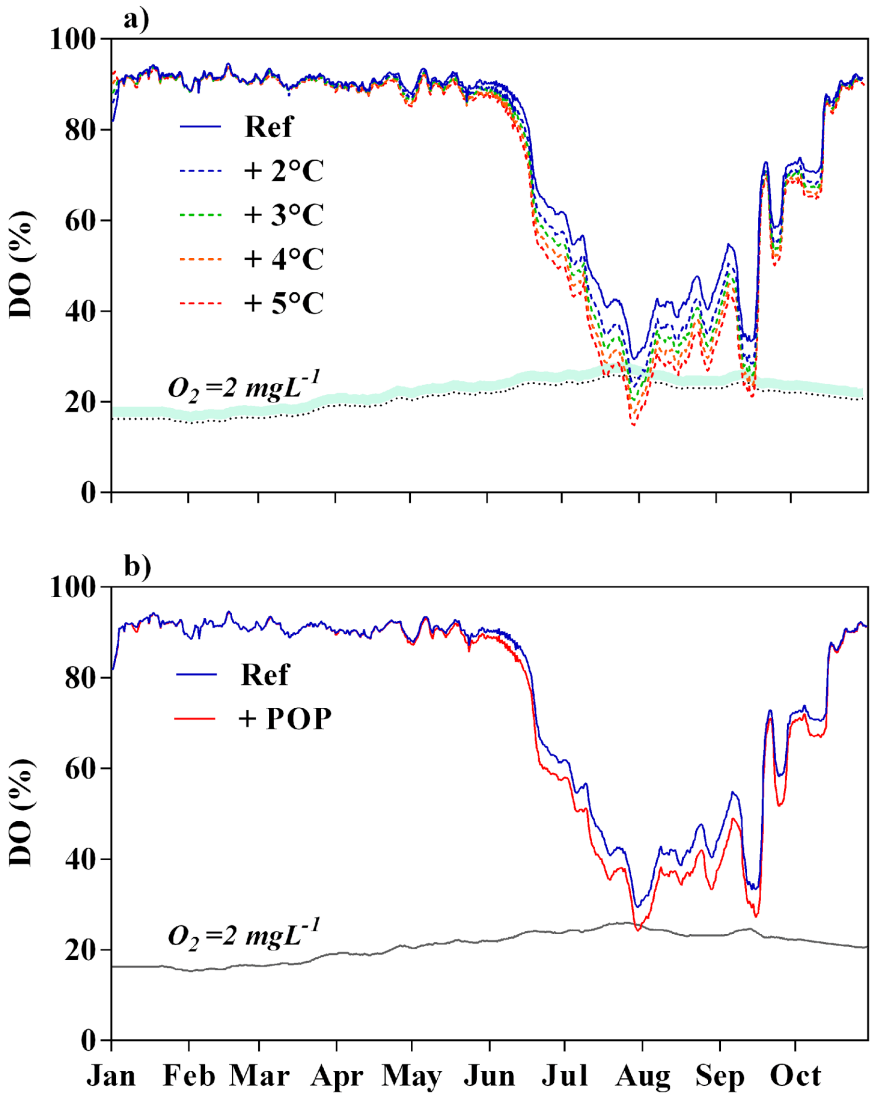
a)
100
80
60
40
20
0
DO (%)
Ref
+ 2°C
+ 3°C
+ 4°C
+ 5°C
O_2 =2 mgL^{-1}
b)
100
80
60
40
20
0
DO (%)
Ref
+ POP
O_2 =2 mgL^{-1}
Jan
Feb
Mar
Apr
May
Jun
Jul
Aug
Sep
Oct

Figure 4:

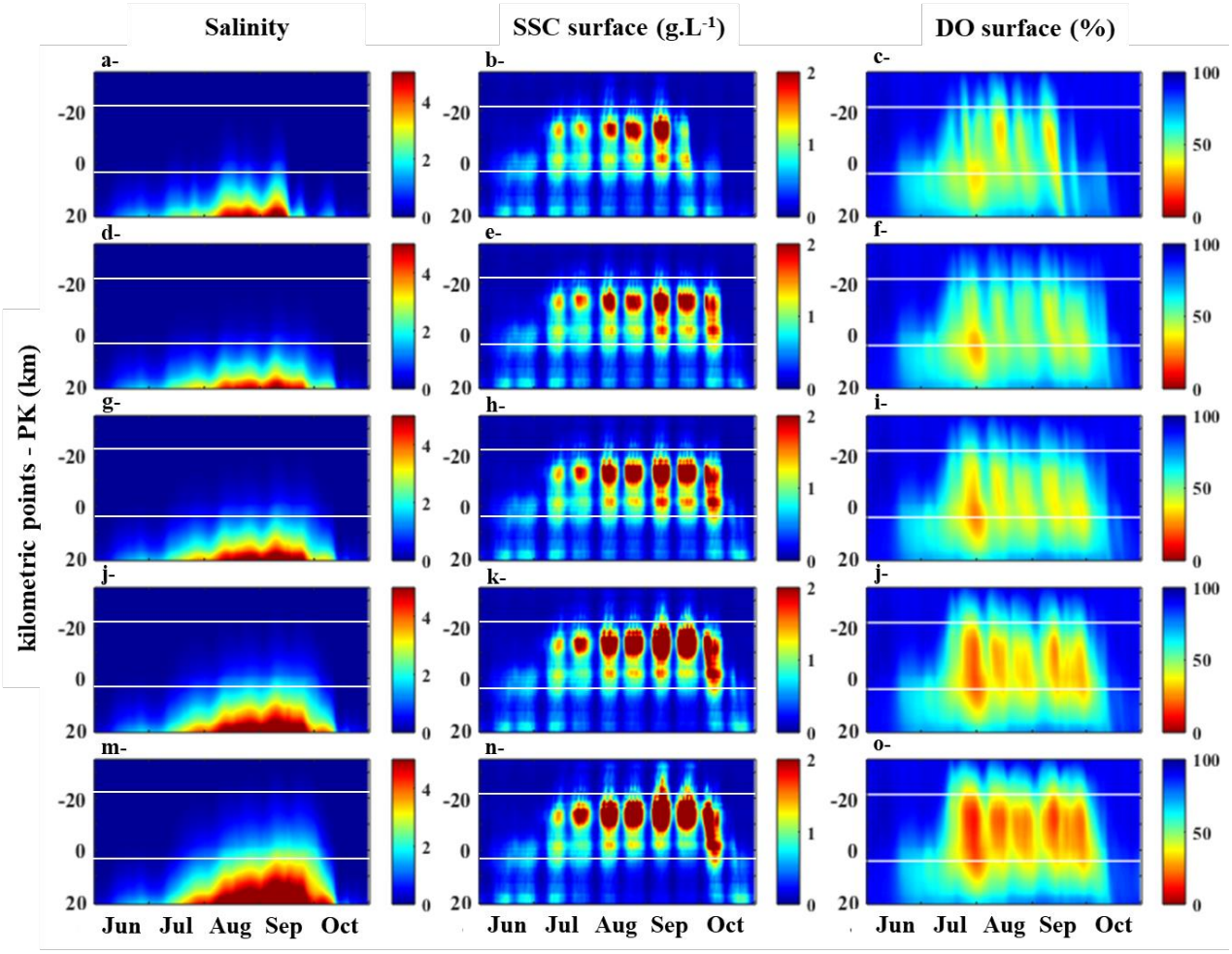
Salinity
SSC surface (g.L-1)
DO surface (%)
kilometric points - PK (km)
a-
b-
c-
d-
e-
f-
g-
h-
i-
j-
k-
j-
m-
n-
o-
-20
0
20
4
2
0
1
100
50
Jun
Jul
Aug
Sep
Oct

Figure 5:

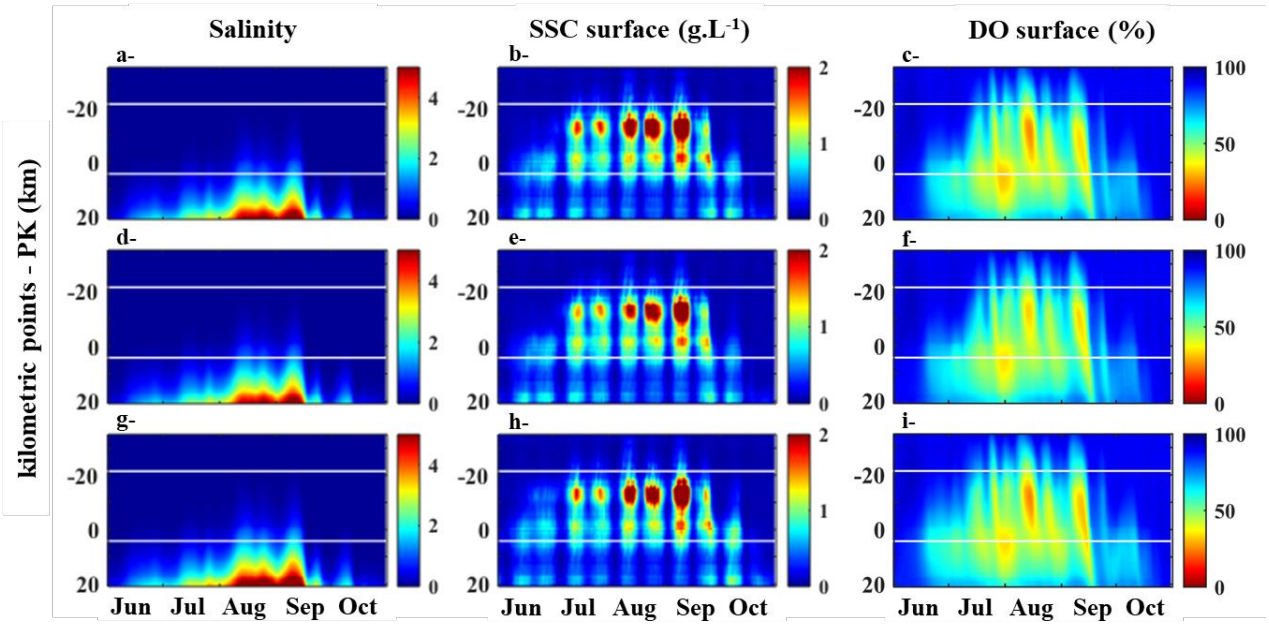
Salinity
SSC surface (g.L-1)
DO surface (%)
kilometric points - PK (km)
a-
b-
c-
d-
e-
f-
g-
h-
i-
-20
0
20
4
2
0
1
100
50
Jun
Jul
Aug
Sep
Oct

Figure 6

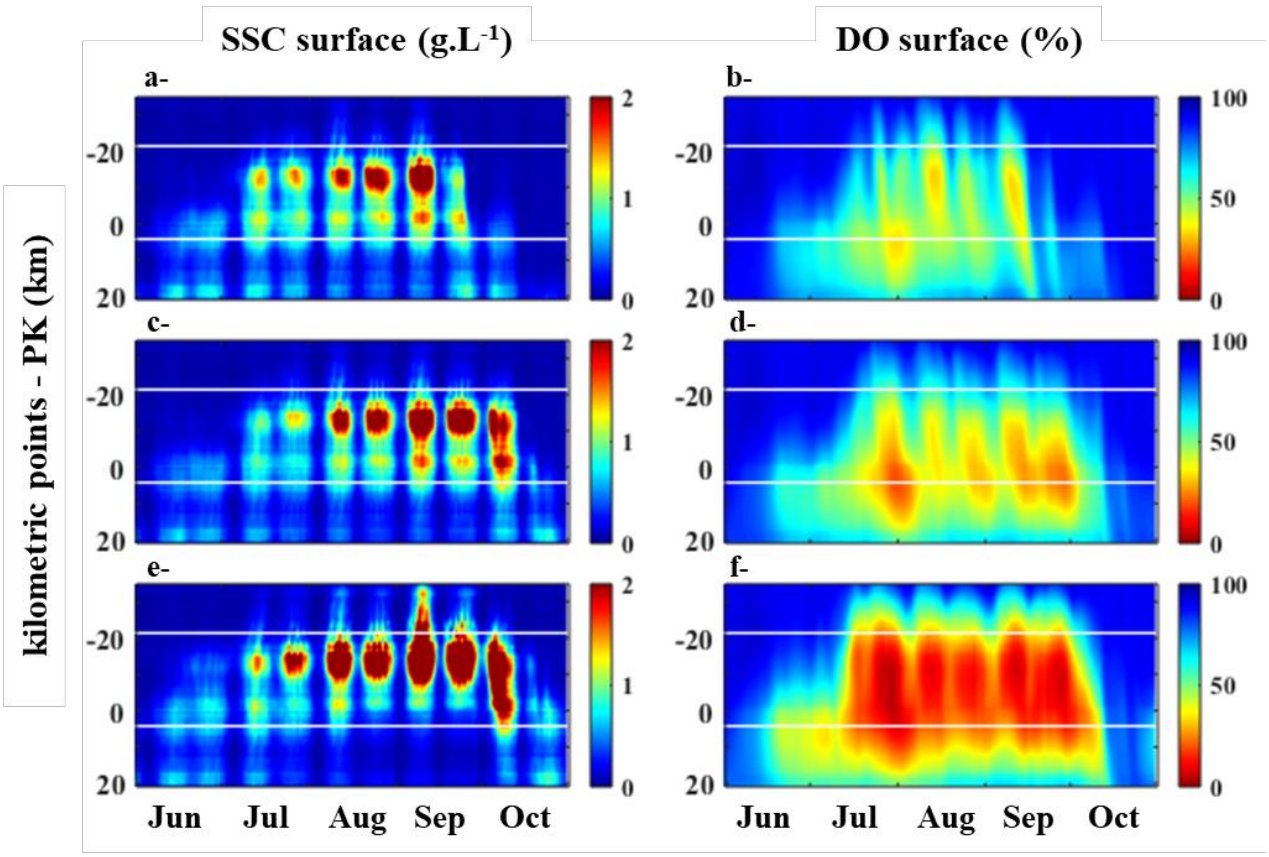
SSC surface (g.L-1)
DO surface (%)
a-
b-
c-
d-
e-
f-
kilometric points - PK (km)
-20
0
20
2
1
0
100
50
Jun
Jul
Aug
Sep
Oct